Title

Pathogenic effects of agrin V1727F mutation are isoform specific and decrease its expression and affinity for HSPGs and LRP4

Journal

Human Molecular Genetics, 28(16)

ISSN

0964-6906

Authors

Rudell, John B
Maselli, Ricardo A
Yarov-Yarovoy, Vladimir
et al.

Publication Date

2019-08-15

DOI

10.1093/hmg/ddz081

Peer reviewed

OXFORD

Human Molecular Genetics, 2019, Vol. 28, No. 16 2648–2658

doi: 10.1093/hmg/ddz081
Advance Access Publication Date: 17 April 2019
General Article

GENERAL ARTICLE

Pathogenic effects of agrin V1727F mutation are isoform specific and decrease its expression and affinity for HSPGs and LRP4

John B. Rudell[1], Ricardo A. Maselli[2], Vladimir Yarov-Yarovoy[1] and Michael J. Ferns[1,3,*]

[1]Department of Physiology and Membrane Biology, University of California Davis, Davis, CA 95616, USA, [2]Department of Neurology, University of California Davis, Davis, CA 95616, USA and [3]Department of Anesthesiology and Pain Medicine, University of California Davis, Davis, CA 95616, USA

*To whom correspondence should be addressed at: Department of Physiology and Membrane Biology, University of California, One Shields Ave, Davis, CA 95616, USA; Tel: (530) 754 4973; Fax: (530) 752 5423; Email: mjferns@ucdavis.edu

Abstract

Agrin is a large extracellular matrix protein whose isoforms differ in their tissue distribution and function. Motoneuron-derived y+z+ agrin regulates the formation of the neuromuscular junction (NMJ), while y−z− agrin is widely expressed and has diverse functions. Previously we identified a missense mutation (V1727F) in the second laminin globular (LG2) domain of agrin that causes severe congenital myasthenic syndrome. Here, we define pathogenic effects of the agrin V1727F mutation that account for the profound dysfunction of the NMJ. First, by expressing agrin variants in heterologous cells, we show that the V1727F mutation reduces the secretion of y+z+ agrin compared to wild type, whereas it has no effect on the secretion of y−z− agrin. Second, we find that the V1727F mutation significantly impairs binding of y+z+ agrin to both heparin and the low-density lipoprotein receptor-related protein 4 (LRP4) coreceptor. Third, molecular modeling of the LG2 domain suggests that the V1727F mutation primarily disrupts the y splice insert, and consistent with this we find that it partially occludes the contribution of the y splice insert to agrin binding to heparin and LRP4. Together, these findings identify several pathogenic effects of the V1727F mutation that reduce its expression and ability to bind heparan sulfate proteoglycan and LRP4 coreceptors involved in the muscle-specific kinase signaling pathway. These defects primarily impair the function of neural y+z+ agrin and combine to cause a severe CMS phenotype, whereas y−z− agrin function in other tissues appears preserved.

Introduction

Congenital myasthenic syndromes (CMSs) are a heterogenous group of genetic disorders characterized by muscle weakness and fatigability due to impaired neuromuscular transmission. CMSs are classified according to the location of the affected protein in the presynaptic terminal, basal lamina or post-synaptic membrane, and to date more than 20 disease-associated genes have been identified (1,2). In most cases the genes encode proteins directly involved in transmission, such as the synthesis of the transmitter acetylcholine (CHAT) or the acetylcholine receptor subunits (CHRN-A1, B1, D and E). However, in 15–20% of cases the genes encode proteins in the agrin signaling pathway that regulate the development and structure of the junction (1,3,4). At

Received: February 21, 2019. **Revised:** March 27, 2019. **Accepted:** April 15, 2019

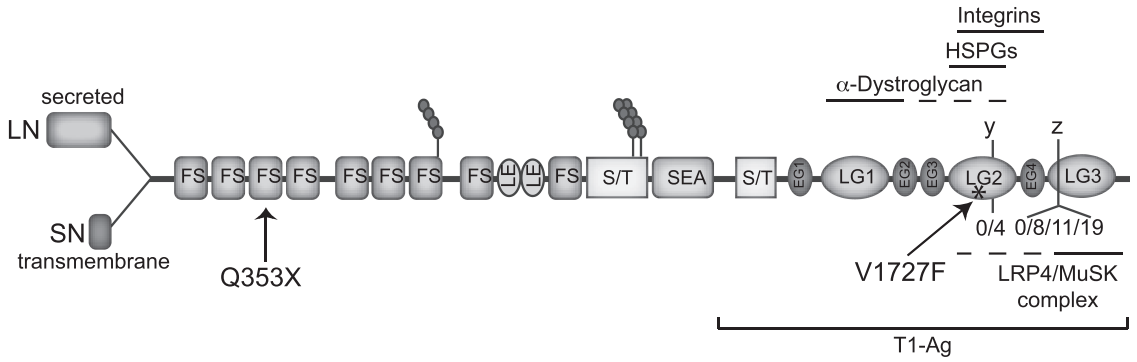

Figure 1. Agrin's structure and position of the mutations. Schematic showing agrin's domain structure, sites of alternative splicing and protein interactions. The Q353X nonsense mutation introduces a premature stop in the third follistatin-like domain. The V1727F missense mutation lies in the LG2 domain. The LG2 domain interacts with HSPGs and integrins, and possibly combines with LG1 to bind αDG, and with LG3 to bind the LRP4/MuSK complex. In addition, splicing at the y site in LG2 regulates binding to HSPGs, and splicing at the z site in LG3 regulates binding to the LRP4/MuSK complex. Functional studies were performed using T1-Ag expression constructs that encompass the C-terminal domains of agrin. FS, follistatin-like domain; S/T, serine–threonine rich domain; EGF, epidermal growth factor-like domain; LG, laminin globular domain.

developing synapses, agrin is released by motor nerve terminals and activates the low-density lipoprotein receptor-related protein 4 (LRP4)/muscle-specific kinase (MuSK) receptor complex on muscle cells (reviewed in 5–7), triggering a signaling pathway that promotes both pre- and post-synaptic differentiation (8–11). Similarly, at mature synapses, agrin deposited in the synaptic basal lamina helps maintain the structure of the neuromuscular junction (NMJ; 12–14). Agrin is essential for development and maintenance of the NMJ, therefore, and its deletion leads to failure of neuromuscular transmission and muscle paralysis (8,14).

Agrin is an atypical synaptogenic factor as it is a large extracellular matrix molecule that occurs in multiple isoforms due to alternative RNA splicing. Agrin's synaptogenic activity is mediated by laminin globular (LG) and epidermal growth factor (EGF)-like repeats near the C-terminus, and splice inserts in these domains regulate its binding to post-synaptic receptors. Most notably, splice inserts at the LG2 domain y site confer binding to heparan sulfate proteoglycans (HSPGs; 15–17), and inserts at the third LG domain (LG3) z site confer binding to the LRP4/MuSK receptor complex (18,19). Indeed, agrin isoforms that contain both y and z inserts (y+z+) are neural specific and are specifically required for NMJ formation (20). In contrast, agrin isoforms that lack y and z inserts (y−z−) are expressed in diverse tissues including skeletal muscle, heart, bladder, blood vessels, immune cells, kidney, cartilage, bone and brain and have alternative functions in these tissues (21,22).

Several cases of CMS due to mutations in AGRN have now been reported (23–28). The mutations lie in several different domains of agrin and likely have a variety of pathogenic effects, giving rise to some variance in the pattern of the disease. Most mutations, however, are concentrated in agrin's C-terminal LG domains. Indeed, we previously identified a missense mutation (V1727F) in the LG2 domain causing severe CMS with profound NMJ defects (28), including smaller presynaptic terminals, fragmented post-synaptic AChR clusters and reduced levels of agrin in the basal lamina. Intriguingly, we found that the LG2 V1727F mutation significantly decreases the ability of z+ agrin to activate MuSK and induce post-synaptic AChR clustering. Here, we investigate the molecular basis by which the LG2 V1727F mutation perturbs agrin expression and signaling and how this leads to the specific CMS.

Results

Agrin's domain structure, splicing and protein interactions are shown in Figure 1, along with the position of the heteroallellic Q353X and V1727F mutations that we found in our patient (28). The nonsense Q353X mutation introduces a premature stop codon in the third follistatin domain and results in a null allele. Consequently, we focused on defining the pathogenic effects of the missense V1727F mutation in the LG2 domain.

Expression of agrin V1727F mutant

Previously we showed that NMJs in the agrin CMS patient were severely disrupted and that agrin immunostaining at the NMJ was reduced compared to controls (28). To define the basis for the decrease in agrin levels we compared the expression and secretion of wild type (WT) and V1727F agrin and tested y+z+ (4,8) and y−z− (0,0) isoforms as both are localized at the NMJ (20,29). As full length agrin is a extracellular matrix proteoglycan that is largely insoluble and difficult to assay (22) we used a C-terminal agrin fragment (Fig. 1) that is soluble and routinely used in assays of receptor binding and AChR clustering (16,19,30).

To assay expression, we transfected COS cells with WT or V1727F 4,8 and 0,0 agrin and then compared the levels of agrin in the cellular fractions and media by immunoblotting with an anti-agrin antibody. As shown in Figure 2A, we found that agrin levels in the cell lysate were similar for WT and V1727F 4,8 and 0,0 agrin isoforms. All constructs appeared as two bands that represent the mature glycosylated protein of ∼140 kD and either a proteolytic breakdown product or immature non-glycosylated core protein of ∼105 kD. Small differences in mobility between y+z+ and y−z− agrin reflect the presence or absence of the 4 and 8 amino-acid splice inserts. Notably, however, we found a striking decrease in V1727F 4,8 agrin levels in the conditioned media compared to WT 4,8 agrin, but no difference in the levels of V1727F 0,0 agrin and WT 0,0 agrin (Fig. 2A). Indeed, quantification of the immunoblots showed that V1727F 4,8 agrin levels in the media were reduced by ∼87% compared to WT 4,8 agrin ($P < 0.0001$, $n = 5$ independent transfection experiments, analysis of variance (ANOVA) and Tukey's test), whereas V1727F 0,0 agrin levels were indistinguishable from WT 0,0 agrin (Fig. 2B). Since WT and V1727F 4,8 and 0,0 agrin were detected at similar

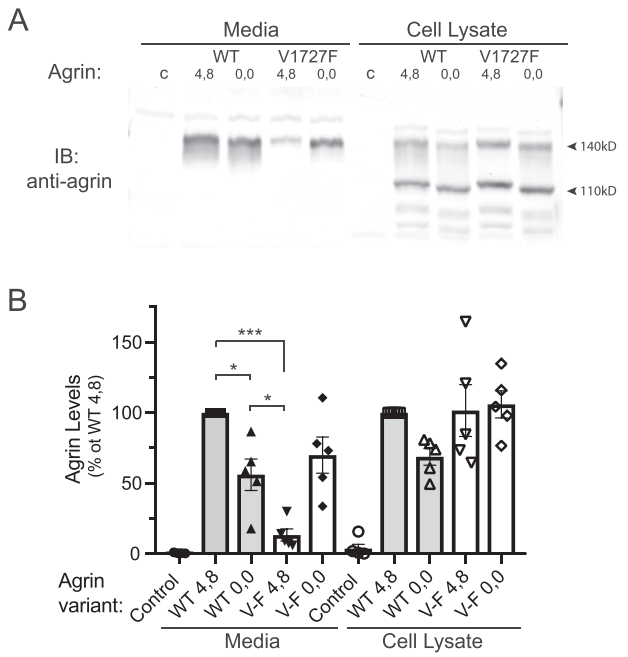

Figure 2. V1727F mutation impairs the secretion of y+z+ agrin. (**A**) Agrin WT and V1727F y4z8 and y0z0 constructs were transiently expressed in COS cells, and their amounts in the media (1/100th of total) and lysate (1/10th of total) were compared by immunoblotting with anti-agrin antibody. All agrin variants were detected at similar levels in the cell lysate and appeared as two bands representing the mature glycosylated protein (~140 kD) and a proteolytic breakdown product or non-glycosylated form (~110 kD). However, V1727F 4,8 agrin was detected at much lower levels in the conditioned media than WT 4,8, WT 0,0 or V1727F 0,0 agrin. (**B**) Quantification showing that the media levels of V1727F 4,8 agrin were significantly reduced compared to both WT 4,8 and 0,0 agrin (***$P < 0.0001$ and $P < 0.005$, respectively, $n = 5$ independent transfection experiments, ANOVA and Tukey test). In contrast, V1727F 0,0 agrin levels were similar to WT 0,0 agrin and not significantly different to WT 4,8 agrin. Note that as WT 4,8 and 0,0 agrin levels differ slightly ($P < 0.05$, $n = 5$, ANOVA and Tukey test), V1727F 4,8 is best compared with WT 4,8 agrin, and V1727F 0,0 with WT 0,0 agrin. In the cell lysate, no significant differences in agrin levels were detected between any of the agrin variants. Thus, the V1727F mutation impairs the secretion of y+z+ but not y−z− agrin from cells into the media.

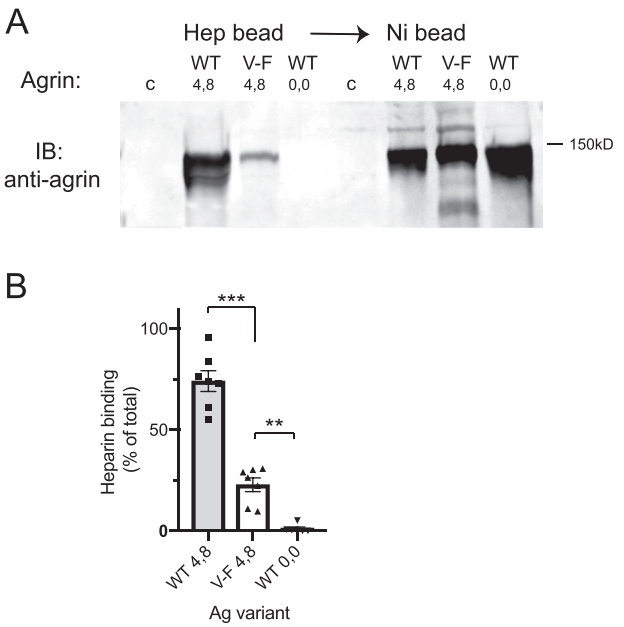

Figure 3. V1727F mutation impairs binding to heparin. (**A**) Conditioned media containing 25 nM WT and V1727F (V-F) agrin were incubated sequentially with heparin Sepharose beads and then with Nickel beads to isolate any remaining His6-tagged agrin. WT 4,8 agrin bound robustly to heparin beads, while V1727F 4,8 agrin bound weakly to heparin and was mostly recovered in the subsequent Nickel bead pulldown. As expected, no heparin binding was detected for WT 0,0 agrin that lacks the y splice insert (KSRK). (**B**) Quantification showing that 23% of V1727F 4,8 agrin was pulled down by heparin beads, compared to 74% of WT 4,8 agrin (***$P < 0.0001$, $n = 7$, ANOVA and Tukey test) and 1% of WT 0,0 agrin ($P < 0.005$, $n = 7$, ANOVA and Tukey test). Thus, the V1727F mutation significantly reduces the binding of y4z8 agrin to heparin.

levels in the cell lysate, these findings suggest that the V1727F mutation does not reduce protein synthesis but rather that it impairs the secretion of 4,8 agrin. Potentially, this may reduce the functional levels of motoneuron-derived y+z+ agrin but not muscle-derived y−z− agrin at the NMJ.

Agrin V1727F–receptor interactions

The V1727F mutation also impairs the ability of y+z+ agrin to activate MuSK and cluster AChRs in the post-synaptic muscle membrane (28). This is somewhat surprising as the mutation lies in the LG2 domain rather than the LG3 domain that is thought to bind the LRP4 coreceptor and thereby activate MuSK signaling (31,32). We investigated, therefore, how the mutation impairs agrin–MuSK signaling and if it involves defective interactions with HSPG or LRP4 coreceptors.

The V1727F mutation lies near the y splice site (aa 1752) in the LG2 domain, where inclusion of a 4 amino-acid (KSRK) insert confers binding to HSPGs and increases agrin's ability to activate MuSK and induce AChR clustering by 5–10-fold (30,33,34). Therefore, we tested whether the mutation might impair binding to HSPGs acting as accessory receptors. To do this, we performed pulldowns of WT and V1727F agrin using heparin-Sepharose beads, and then isolated any unbound His6-tagged agrin using Nickel beads. As expected, we observed robust binding of WT 4,8 agrin to heparin beads, but no binding of WT 0,0 agrin (Fig. 3). Most importantly, we found that binding of V1727F 4,8 agrin to heparin was reduced by ~70% compared to WT 4,8 agrin ($P < 0.0001$, $n = 7$, ANOVA and Tukey's test). Thus, the V1727F mutation partially occludes the effect of the 4 amino-acid (KSRK) insert on heparin binding and thereby impairs interaction with HSPG accessory receptors. Together with previous works (15–17), this suggests that agrin–HSPG receptor interactions likely participate in LRP4/MuSK activation and/or downstream AChR clustering.

Next, we tested whether the V1727F mutation impairs agrin binding to the LRP4 coreceptor. For this, we expressed full-length LRP4 in heterologous human embryonic kidney (HEK) cells, which presumably lack other agrin receptors involved in synapse formation. The transfected HEK cells were incubated with 10 nM WT or V1727F 4,8 agrin for 30 min, and then immunostained for bound exogenous agrin using anti-agrin (mAb131) or anti-Flag antibody. As expected, we observed robust binding of WT 4,8 agrin to HEK cells expressing LRP4 but not to control (sham-transfected) cells (Fig. 4A). In contrast, we detected only weak binding of V1727F 4,8 agrin to LRP4 expressing cells (Fig. 4A). No agrin binding was detected in cells treated with WT 0,0 agrin that has minimal affinity for LRP4, or in cells treated with control media lacking agrin, confirming that agrin binding is LRP4-dependent and neural (y+z+) agrin specific. Thus, y+z+ agrin binding to LRP4 is significantly reduced in the V1727F mutant.

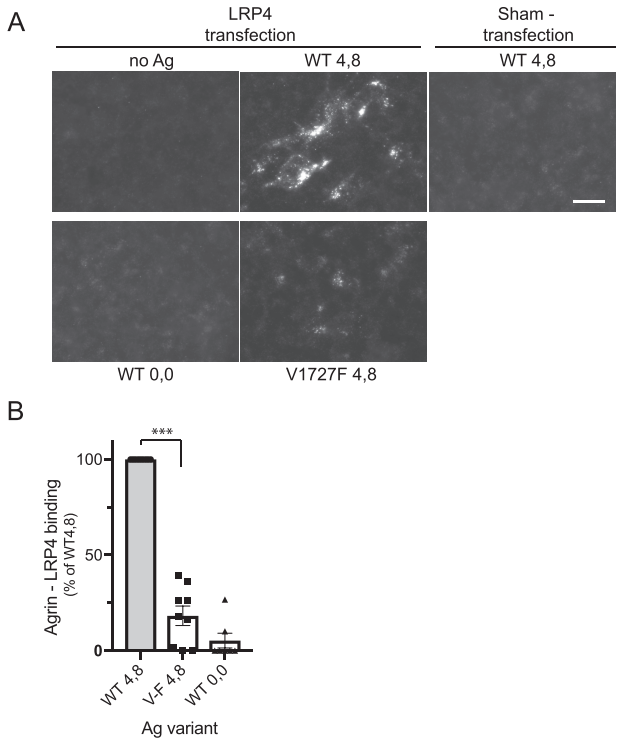

Figure 4. Agrin binding to LRP4 is inhibited by V1727F mutation. (**A**) HEK cells were transiently transfected with full-length LRP4 or empty vector and incubated with 10 nM WT or V1727F agrin for 30 min. After washing, the cells were fixed in methanol and bound agrin was detected with anti-agrin antibody (mAb131) and AF594-conjugated secondary antibody. Images were acquired using identical exposure times. Agrin 4,8 binding was clearly evident to LRP4-expressing cells but not sham-transfected cells and was greatly reduced for V1727F compared to WT 4,8 agrin. No WT 0,0 agrin binding to LRP4 expressing cells was detected, confirming that the interaction is z+ isoform specific. Scale bar = 10 μm. (**B**) Binding of WT and V1727F agrin to LRP4 was quantified using an On-Cell Western assay. HEK cells expressing LRP4 were incubated with 10 nM agrin for 30 min, and then bound agrin was detected with anti-agrin antibody and IR680-conjugated secondary antibody and quantified with an Odyssey scanner. Total values were corrected for non-specific binding, measured using sham-transfected cells. Binding of V1727F 4,8 agrin to LRP4 was significantly reduced compared to WT 4,8 agrin (by 82%; $P < 0.0001$, $n = 9$ independent transfection experiments, ANOVA and Tukey test) and was similar to that of WT 0,0 agrin.

To quantitatively compare WT and V1727F agrin binding to the LRP4 coreceptor we utilized an On-cell Western assay. HEK cells expressing LRP4 were incubated with 10 nM agrin for 30 min, washed, fixed and permeabilized in cold methanol, and bound agrin was then detected with anti-agrin antibody (mAb131) and IR680-conjugated anti-mouse secondary antibody. Non-specific binding was determined using sham-transfected cells, and signals were visualized with an Odyssey Fc imager and quantified with Image Studio software. Consistent with the immunostaining experiments, we found that V1727F 4,8 agrin binding to LRP4 was ~80% lower than that of WT 4,8 agrin ($P < 0.0001$, $n = 9$, ANOVA and Tukey's test), and similar to WT 0,0 agrin (Fig. 4B). Together, these findings demonstrate that the V1727F mutation significantly impairs agrin binding to LRP4, suggesting that the LG2 domain contributes (either directly or indirectly) to the interaction. This likely contributes to the decreased ability of V1727F y+z+ agrin to activate MuSK and its downstream signaling pathway.

Unexpectedly, we also found that agrin–LRP4 binding was followed by internalization of the proteins from the cell surface. This was clearly evident in time course experiments where HEK cells expressing LRP4-mCherry were treated with WT 4,8 agrin for 5, 10 or 30 min (Supplementary Material, Fig. 1). At 5 min, agrin was detected predominantly on the cell surface or in small vesicles that partially colocalized with LRP4-mCherry. However, at 10–30 min agrin was mostly detected in large intracellular puncta that were not colocalized with LRP4. Thus, following internalization, agrin accumulates in large intracellular vesicles, and LRP4 is either trafficked to a distinct intracellular compartment or recycled back to the plasma membrane.

Structural effects of LG2 V1727F mutation

To gain structural insights into how the V1727F mutation impacts agrin function we modeled the mutation using the mouse agrin LG2 x-ray structure (PDB ID: 3PVE) as described in Materials and Methods. As shown in Figure 5A and B, the LG domain consists of a beta sheet sandwich and the connecting loops on the upper edge constitute the hypervariable surface that commonly mediates protein interactions (35). Valine 1727 lies in the β8 strand and the y splice site lies in the β10–11 loop, on the lateral edge of the LG2 domain. As valine's sidechains face inward, substitution with the bulkier phenylalanine residue likely alters the packing of the beta strands. Consequently, we used Rosetta structural modeling software to examine how this might impact the LG2 domain structure. First, we modeled the KSRK insert at the y splice site, which was not present in the LG2 crystal structure. The consensus models showed that this positively charged insert forms a short outward-facing loop at the edge of the beta sheet sandwich (Fig. 5A), readily accessible for binding by HSPGs. Second, we generated relaxed models of the WT and V1727F LG2 domains, to assess possible structural changes due to the mutation. The 10 lowest energy models for the WT and V1727F LG2 domain suggest that the mutation causes minimal change in the beta sheets but probable shifts in the position of loop regions on the hypervariable surface (Fig. 5C and D). Most notable is a lateral shift in the position of the β10–11 loop, which contains the KSRK insert. This shift of the KSRK loop on the domain edge could impair heparin binding and other interactions of the LG domain. Intriguingly, another CMS mutation (G1709R) shown to destabilize the NMJ (23) lies in the adjacent β6–7 loop on the hypervariable surface (Fig. 5E). Moreover, substitution of glycine (1709) with arginine in our model shows that its long sidechains clash with the KSRK loop and could alter its position (Fig. 5F).

Our structural modeling suggests that the pathogenic effects of the V1727F mutation involve disrupted structure and function of the y splice insert. To assess this, we compared the functional effects of the V1727F mutation on individual agrin y and z splice variants. First, in assays of agrin expression in heterologous COS cells, we found that the V1727F mutation greatly decreased secretion of the 4,8 and 4,0 isoforms, but not the 0,8 and 0,0 isoforms (Fig. 6A). Second, we assayed agrin binding to heparin conferred by the y4 insert (Fig. 6B and C) and found that the V1727F mutation inhibited binding of the 4,8 and 4,0 isoforms by 64% and 44%, respectively, compared to WT agrin ($P < 0.0001$ and $P < 0.001$, $n = 4$–7, ANOVA and Tukey's test). Thus, the mutation causes significant defects in agrin isoforms that contain the y4 insert. The analysis of the G1709R mutation that lies adjacent to the y insert revealed milder functional defects. The G1709R mutation did not reduce agrin protein levels in the cell lysate or media (Fig. 6A), but decreased binding of the 4,8 isoform to heparin by 29% ($P = 0.01$, ANOVA and Tukey's test; Fig. 6B and C).

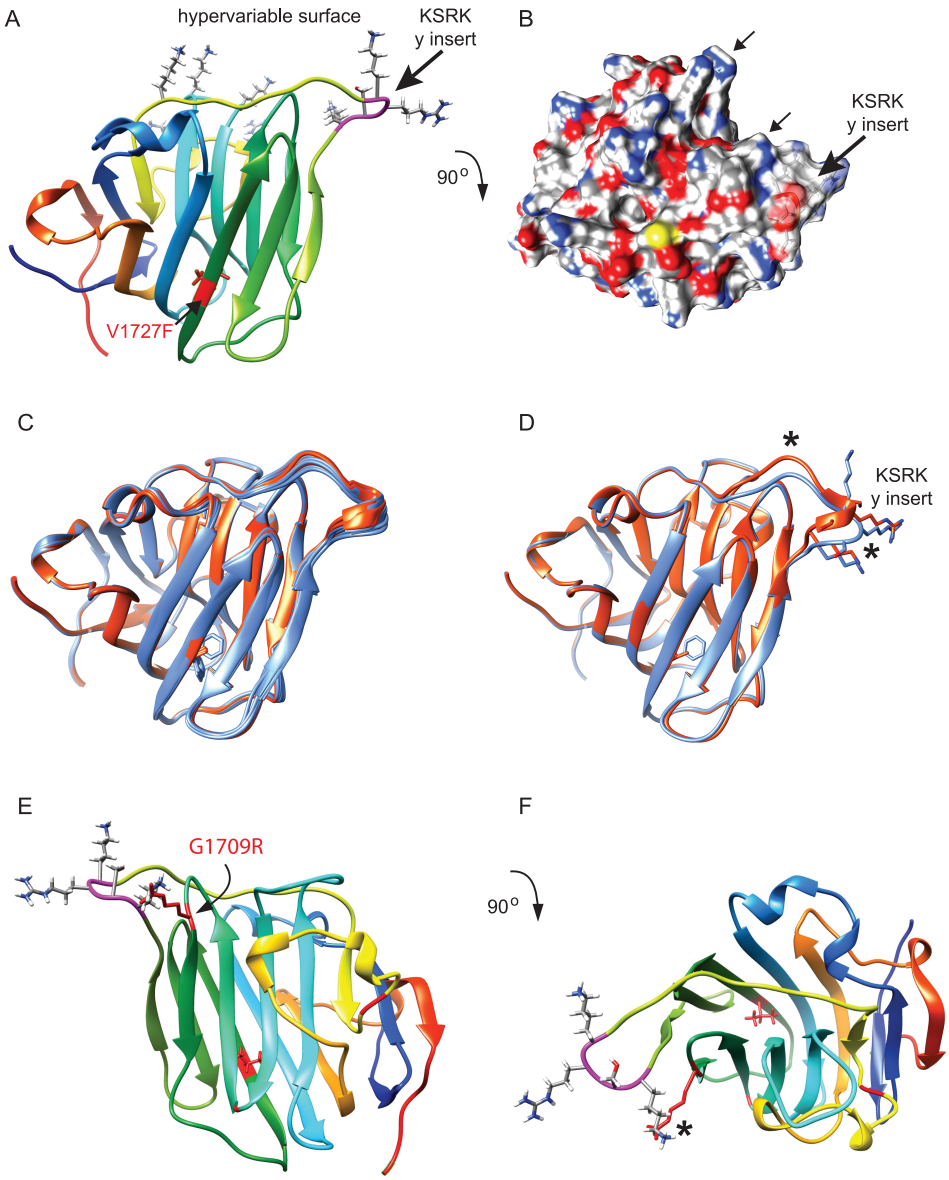

Figure 5. Structural effects of LG2 domain V1727F mutation. **(A)** The mouse LG2 domain structure (PDB ID: 3PVE) is composed of a beta sheet sandwich with connecting loops that form a hypervariable surface (top), which often mediates LG domain interactions with their binding partners. The KSRK insert at the y splice site (pink) was modeled using Rosetta structural modeling software and forms an outward facing loop on the edge of the hypervariable surface (black arrow). The positively charged residues on the hypervariable surface are shown with their sidechains in stick representation. The V1727F mutation is located in beta strand 8 and is depicted in red. **(B)** Electrostatic surface representation showing the top surface of LG2 (rotated 90° from A). The KSRK insert is indicated by the large black arrow and introduces additional positively charged residues (blue) on the hypervariable surface (arrows). **(C)** Comparison of multiple relaxed models of WT (orange) and V1727F (blue) LG2 domain structures. **(D)** Single WT and V1727F models showing that their structures differ most in the loops on the hypervariable surface (asterisks), with significant shifts in some loops in V1727F (blue) compared to WT (orange). In particular, the KSRK insert loop is shifted laterally in the mutant structure. **(E)** Rear surface of the LG2 domain (from A) showing the G1709R mutation (red) in the β6–7 loop that lies immediately adjacent to the KSRK insert (pink). **(F)** Top surface of the LG2 domain (rotated 90° from E) showing arginine's long sidechains (red) that may clash with the KSRK loop and thereby alter its position.

Conversely, substitution of glycine with the positively charged arginine residue did not confer heparin binding to the 0,0 isoform. Thus, the G1709R mutation may also partially disrupt y splice site function and this could contribute to its pathogenic effects.

Finally, we assayed the effect of the y4 insert and mutation on agrin binding to LRP4. Surprisingly, we found that LRP4 binding was significantly reduced for WT 0,8 compared to WT 4,8 agrin (Fig. 7A and B), indicating that the y4 insert contributes (either directly or indirectly) to the apparent affinity of the LRP4 interaction. Thus, the decreased binding of V1727F 4,8 agrin to LRP4 approximates that observed for WT 0,8 agrin (Fig. 7B).

In summary, we find that V1727F 4,8 agrin binding to both HSPGs and LRP4 resembles that of WT 0,8 agrin. This supports our structural modeling and indicates that the mutation partially occludes the function of the LG2 domain y splice insert. As z inserts always occur in combination with y inserts (36), this will impact all neural y+z+ agrin isoforms.

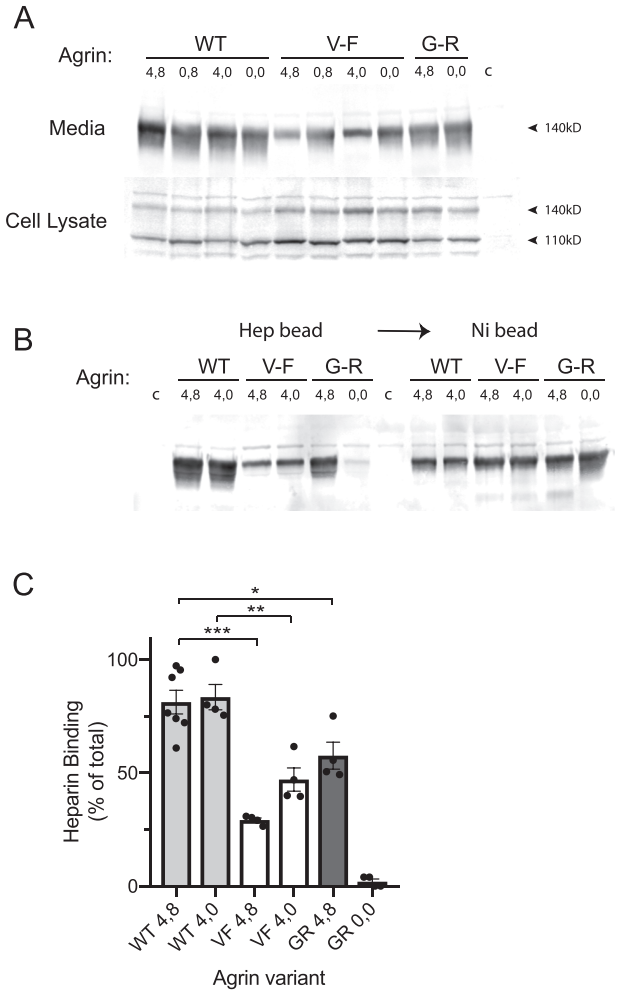

Figure 6. Isoform-specific effects of V1727F mutation on agrin function. (**A**) Agrin splice variants were expressed in COS cells in WT form or with V1727F or G1709R mutations, and their levels in the media and cell lysate were compared by immunoblotting with anti-agrin antibody. For V1727F mutants, media levels were significantly reduced for the 4,8 and 4,0 isoforms but not the 0,8 and 0,0 isoforms. Media levels of the G1709R mutants were similar to WT, and all variants were detected at similar levels in the cell lysate. Thus, the V1727F mutation impairs the secretion of agrin y4 isoforms into the media. (**B**) Pulldowns of agrin variants were performed sequentially using heparin- and then Nickel-beads. The amount of agrin that bound to heparin beads was significantly reduced for V1727F 4,8 and 4,0 isoforms compared to WT 4,8 and 4,0 agrin, and modestly reduced for G1709R 4,8 agrin. (**C**) Quantification showing that ~82% of WT 4,8 and 4,0 agrin were pulled down by heparin beads, compared to only 29% of V1727F 4,8 and 47% of V1727F 4,0 agrin ($P < 0.0001$ and $P < 0.001$, respectively, $n = 4$–7, ANOVA and Tukey test). Heparin binding was also modestly reduced for G1709R 4,8 agrin (58%, $P = 0.01$, $n = 4$, ANOVA and Tukey test) and no binding was detected for G1709R 0,0 agrin. Thus, the V1727F and G1709R mutations both reduce y4-dependent binding to heparin.

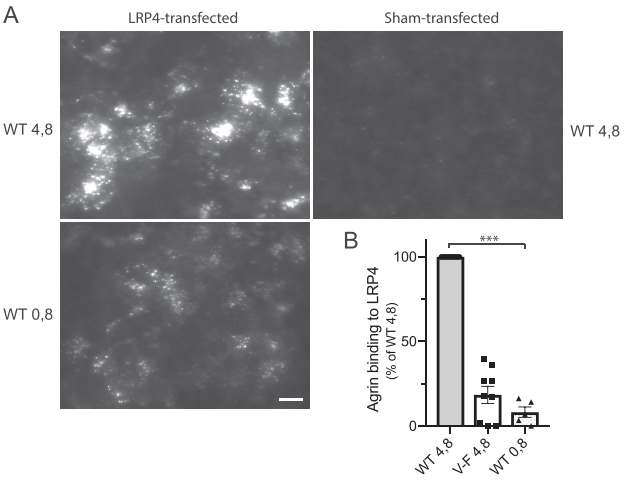

Figure 7. Agrin-LRP4 binding is enhanced by the y4 insert. (**A**) HEK cells transfected with full-length LRP4 or empty vector were incubated with 10 nM WT 4,8 or 0,8 agrin for 30 min. Bound agrin was detected with anti-agrin antibody and images were acquired using identical exposure times. LRP4 binding was significantly lower for the 0,8 isoform compared to the 4,8 isoform. Scale bar = 10 µm. (**B**) Quantification from On-cell Western assays shows that WT 0,8 agrin binds LRP4 at significantly lower levels than WT 4,8 agrin (decrease of 92%, $P < 0.0001$, $n = 9$, ANOVA and Tukey test), and at levels similar to V1727F 4,8 agrin.

Discussion

In this study we identify several pathogenic effects of the agrin V1727F mutation that impair agrin function at the NMJ. These defects mostly impact neural y+z+ agrin and thereby account for the specific and severe CMS phenotype.

Agrin expression

The first pathogenic mechanism identified in this study is that the V1727F mutation inhibits the secretion of y+z+ soluble agrin expressed in heterologous cells. This striking defect was limited to y+ isoforms and likely involves structural changes in the y4 insert as suggested by our molecular modeling studies. Such changes could then disrupt the conformation of y+z+ isoforms and thereby impair their trafficking and secretion. Consistent with this, both y and z splice inserts are thought to regulate the conformation of neural agrin, as they confer binding of a neural agrin-specific antibody (mAb86) (37) and reduce binding to dystroglycan mediated by the LG1–2 domains (16). Moreover, the V1727F mutation disrupts this conformation, as it decreases binding to mAb86 and increases binding to dystroglycan (28). It seems likely that the mutation also alters the conformation of full-length y+z+ agrin expressed in motoneurons and y+z− agrin expressed in muscle and that it could thereby impair their secretion and functional expression. Consequently, we propose that V1727F contributes along with the Q353X null mutation to the reduced agrin levels at the NMJ and to the CMS phenotype (28). In particular, reduced y+z+ agrin levels would impair agrin signaling critical for NMJ formation and maintenance.

Our finding that the V1727F mutation reduces the functional levels of y+z+ but not y−z− agrin has another important implication. Agrin isoforms lacking y and z inserts (y−z−) are expressed in diverse tissues, including skeletal muscle, heart, bladder, blood vessels, kidney, cartilage, bone and brain and have many proposed functions (21,22). Most notably, this includes roles in erythropoiesis (38), hematopoiesis (39,40), T lymphocyte activation (41,42), cartilage formation and bone growth (43,44) and blood–brain–barrier function (45). Indeed, transgenic mice that express agrin only in motor neurons are considerably smaller than control littermates and have a mean survival time of only 50 days (46). Our findings predict that y–z– agrin levels are only moderately reduced in the patient, however, due to the Q353X but not the V1727F mutation. Thus, y−z− agrin function may be largely preserved, which could account for the apparent absence of defects in other tissues in the patient (such as anemia, immune dysfunction and skeletal abnormalities).

Agrin–receptor binding

A second pathogenic mechanism that we identified is that the V1727F mutation impairs binding to two post-synaptic receptors, HSPGs and LRP4. These defective interactions likely account for the decreased ability of agrin V1727F to activate MuSK and induce post-synaptic AChR clustering (28).

In the case of HSPGs, we found that the V1727F mutation caused an ∼80% reduction in y4z8 agrin binding to heparin. An agrin–proteoglycan interaction has been implicated in neuromuscular synapse formation, as the y splice insert conferring heparin binding increases agrin's synaptogenic activity 5–10-fold (30,33,34), whereas agrin's activity is reduced in muscle cell lines with defective proteoglycan synthesis (30) or treated with heparinase (47). Although genetic experiments in mice demonstrate that the y insert is not absolutely required for agrin function (20), these findings indicate that an agrin–proteoglycan interaction enhances agrin's activity and this is presumably defective in the V1727F mutant. Most likely, this involves proteoglycans acting as accessory receptors that facilitate agrin binding to the LRP4/MuSK signaling complex, as proteoglycans commonly perform this role in other signaling systems (48,49). Additionally, agrin–proteoglycan interactions could stabilize later stages of post-synaptic differentiation via structural mechanisms (15). Several secreted and transmembrane proteoglycans have been implicated in vertebrate or Drosophila NMJ formation, including muscle agrin, perlecan, biglycan, syndecan and glypican (50), and a recent study demonstrated that agrin binds preferentially to moderately charged heparan sulfate oligosaccharides on proteoglycans (47). However, the identity of the proteoglycan involved in agrin signaling remains unknown.

Another defect was impaired interaction with LRP4, with binding of V1727F agrin reduced by ∼82% compared to WT y+z+ agrin. This is surprising as the V1727F mutation lies in the LG2 domain and previous studies have identified the LG3 domain as the minimal fragment to bind LRP4, activate MuSK and induce AChR clustering (31,32). On the other hand, the C-terminal LG3 fragment is several hundred-fold less potent than larger agrin constructs that include the LG2 domain (32), and binding of antibodies and heparin to the LG2 domain inhibits agrin-induced MuSK phosphorylation and AChR aggregation (33,37). Together, these findings demonstrate that the LG2 domain plays an important role in LRP4 binding and MuSK activation, although the molecular mechanism remains unclear. One possibility is that the LG2 domain forms an additional binding interface with LRP4, perhaps interacting with the 3 LDLa and 2 EGF repeats that contribute to agrin binding along with the first beta propeller domain (51). A second possibility is that the LG2 domain affects the conformation and availability of the LG3 domain for LRP4 binding. Potentially, the V1727F mutation could alter this conformation (28) and decrease the apparent affinity for LRP4. A third possibility is that the LG2 domain binds a coreceptor, such as a HSPG, that increases the local concentration of agrin and facilitates its binding to LRP4. This is consistent with the reduced LRP4 binding of WT 0,8 compared to WT 4,8 agrin but requires that a proteoglycan coreceptor is endogenously expressed in HEK cells.

In summary, we find that the agrin V1727F mutation significantly impairs binding to both LRP4 and HSPGs, by 4–5-fold in each case. As the V1727F mutation decreases MuSK activation by ∼10-fold and AChR clustering by ∼100-fold (28), we propose that the defects in interactions with LRP4 and HSPG may combine to significantly impair agrin–MuSK signaling and that this is a second major determinant of the pathogenesis of the disease. Notably, these functional defects are greatest for neural y4z8 agrin, where the mutation partially occludes both the y4-dependent binding to HSPGs and the y4/z8-dependent binding to LRP4. Thus, as for expression, the pathogenic effects of the V1727F mutation on receptor binding largely impact y+z+ neural agrin isoforms.

Molecular basis for pathogenic effects of V1727F mutation

Our findings demonstrate that the agrin LG2 domain, as well as the LG3 domain, is critical for agrin's receptor interactions and synapse-organizing activity. Interestingly, LG domain repeats in other molecules like neurexin and perlecan mediate receptor interactions with many similarities to those of agrin (21,35) and give potential insight into the pathogenic basis of the V1727F mutation. Most notably, their receptor interactions usually involve the LG domain hypervariable surface (35), with adjacent LG domains either combining to bind a single receptor (52) or acting independently to bind multiple receptors (53). Moreover, as in agrin, some interactions are regulated by splicing and/or conformational changes in the LG domain repeats (35). Thus, the multiple defects that we observed for the V1727F mutant (see sections above) are consistent with the agrin LG2 and LG3 domains acting in a combinatorial and highly regulated manner with their post-synaptic receptors (34).

Our structural modeling provides further clues as to the pathogenic mechanism of the agrin V1727F mutation. Based on the mouse agrin LG2 domain structure, valine 1727 lies in a beta sheet (Fig. 5A) and substitution with a bulkier phenylalanine residue likely disrupts the packing of the beta strands and impacts the domain structure. Indeed, our modeling of the mutant LG2 domain using Rosetta predicts changes in the loops on the hypervariable surface, and most notably in the β10–11 loop that contains the y splice site insert KSRK. Consistent with this, we found that the V1727F mutation impaired both secretion of y4 agrin and y4 dependent binding to HSPGs. This suggests the following molecular model for how the V1727F mutation might disrupt the structure and function of y+z+ agrin (Fig. 8). Previous studies show that the y and z splice inserts induce a conformational change in agrin and also contribute to HSPG and LRP4 binding, respectively. We propose (i) that the V1727F mutation impairs this conformational change, resulting in a structure that is intermediary between y+z+ and y−z− agrin. This decreases binding to LRP4 and neural agrin-specific antibody mAb86, but increases binding to alpha dystroglycan (αDG). We further propose (ii) that the V1727F mutation distorts the y splice insert on the LG2 hypervariable surface and thereby impairs binding to HSPGs. This loss of HSPG coreceptor function further decreases agrin–LRP4/MuSK interaction. Together, these molecular defects combine to significantly impair agrin–MuSK signaling and disrupt the structure and function of the NMJ.

In summary, we have identified multiple pathogenic effects of the agrin V1727F mutation that decrease its functional levels and ability to bind HSPG and LRP4 coreceptors critical for MuSK signaling and synaptic differentiation. These deficits largely impair the function of neural y4z8 agrin and consequently account for the severe CMS observed in the patient and the absence of deficits in other tissues.

Materials and Methods

Agrin constructs and production of soluble agrin

Previously, we reported two novel, heteroallelic mutations in AGRN: a nonsense mutation p.Q353X and a missense mutation

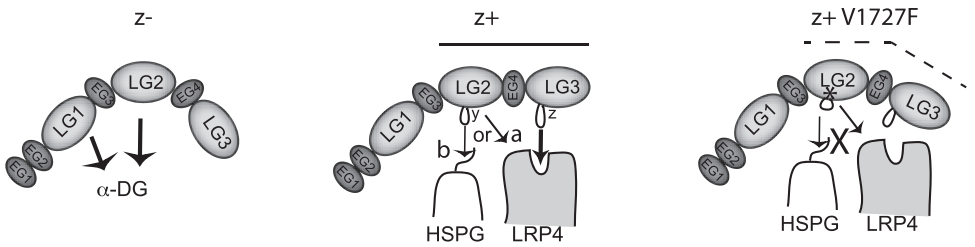

Figure 8. Model for pathogenic effects of V1727F mutation on agrin function. A molecular model for how the V1727F mutation selectively disrupts the conformation of y+z+ agrin and its receptor interactions. In y−z− agrin, the conformation of the LG1–3 domains favor binding to αDG. In y+z+ agrin, the y and z inserts (loops) induce a change in conformation (straight line) and contribute to HSPG and LRP4 binding, respectively. We propose that agrin binding to LRP4 (and subsequent MuSK activation) involves the LG2 as well as the LG3 domain. Potentially, the LG2 domain could bind directly to LRP4 (a) or to a HSPG accessory receptor (b) that indirectly facilitates agrin binding to LRP4. In the V1727F mutant (asterisk), the conformation is intermediary between y+z+ and y−z− agrin (angled line) and binding to HSPG and LRP4 is impaired (X).

p.V1727F (using GenBank NM_198576.2 and NP_940978.2 as reference; 28). To express the agrin variants we used a pFlag-CMV1 vector encoding the C-terminal half of rat agrin (Fig. 1), which has 88% identity to the human sequence (28). This construct (denoted as T1-Ag) contains amino-terminal Flag and His6 epitope tags but is otherwise equivalent to the C-Ag construct used previously to generate soluble agrin for MuSK activation and AChR clustering assays (30,33). The y+z+ (y4z8) and y−z− (y0z0) splice variants and the V1727F mutation were generated and characterized in previous studies (28,30).

To generate soluble agrin, we transfected COS cells with the T1-Ag constructs using Fugene and collected the conditioned media after 2–3 days. We then determined the concentration of agrin by immunoblotting with anti-agrin antibody and comparing the signal with a known amount of purified agrin, as previously described (30). Agrin was used at a concentration of ∼25 nM for heparin binding and 10 nM for LRP4 binding assays.

Agrin expression

To assay agrin expression, we transfected COS cells with T1-Ag constructs encoding WT and V1727F y+z+ (y4z8) and y−z− (y0z0) agrin. After 1 day of expression, we collected the conditioned media containing soluble, secreted agrin. The transfected cells were then rinsed in PBS, collected and extracted in phosphate buffer containing 0.5% Triton, 5 mM EDTA and Halt protease inhibitor cocktail (Thermo Fisher Scientific, Waltham, MA). Samples of the conditioned media (1/100th of total) and lysate (1/10th of total) were run on 7% polyacrylamide gels and immunoblotted with rabbit anti-agrin antibody and IR680-conjugated secondary antibody. Signals were visualized with an Odyssey Fc imager and quantified with Image Studio software.

Agrin–heparin binding

To assay heparin binding, agrin WT and V1727F conditioned media were diluted with Hepes buffer (20 mM Hepes, 150 mM NaCl, pH 7.3) to a concentration of 25 nM and incubated with 50 µl of heparin-Sepharose beads for 4 h at 4°C. The beads were then pelleted, washed three times in Hepes buffer and bound agrin eluted by boiling in SDS-loading buffer. Unbound (His6-tagged) agrin was then sequentially isolated from the media supernatant by incubating with 30 µl of Ni-beads (Talon metal affinity resin, Clontech, Palo Alto, CA) for 2 h at 4°C. The beads were pelleted, washed three times in Hepes buffer plus 5 mM imidazole and bound agrin eluted as above. The heparin- and Ni-bead isolates were run on a 7% polyacrylamide gel and detected by immunoblotting with anti-agrin antibody.

Agrin–LRP4 binding

To assay LRP4 binding, we transfected HEK cells grown on 8-well glass chamber slides (Lab-Tek, Rochester, NY) with pcDNA3 vector encoding full-length LRP4 (gift of Dr Joachim Herz, UT Southwestern). After 2 days of expression, we incubated the live cells with 50 nM WT or V1727F agrin for 30 min. After washing, the cells were fixed in methanol and bound agrin was detected with monoclonal antibody (mAb131) that is specific for rat agrin and AF594-conjugated secondary antibody. The labeled culture slides were viewed with a Zeiss Axioplan 2 IE fluorescence microscope, and digital images were acquired with an Axiocam MRM camera and Axiovision software. Identical exposure times were used for all conditions. In some experiments, we detected agrin binding with an anti-Flag antibody or utilized an LRP4 construct tagged with mCherry (gift of Dr Steven Burden, New York University) in order to assess colocalization of agrin and LRP4.

Binding of WT and V1727F agrin to LRP4 was quantified using an On-cell Western assay. These experiments were performed as described above, except that bound agrin was detected with anti-agrin antibody (mAb131) and IR680-conjugated anti-mouse secondary antibody. Signals were visualized with an Odyssey Fc imager, and total binding was quantified for each well using Image Studio software. Non-specific binding was determined using sham-transfected cells and subtracted from the total values.

Structural modeling of agrin

Homology modeling of agrin structure region from S1633 to G1819 was performed using Rosetta structural modeling software (54–56) and x-ray structure of the G2 domain of agrin from *Mus musculus* (PDB ID: 3PVE) as a template. Missing loop regions in the 3PVE template structure (between residues F1654 and M1662 and also T1684 and G1686) and the KSRK insert site (between residues P1751 and V1756) were modeled *de novo* using the cyclic coordinate descent loop modeling approach (57). A total of 10 000 agrin models were generated and the 1000 lowest energy models were clustered (58) with a root mean square deviation threshold of 0.5 Å between Cα atoms. The top cluster agrin model was used to generate all atom relaxed models of the WT and V1727F mutant using Rosetta relax application (59–62). All structural figures were generated using the UCSF Chimera

package (63). Structural coordinates of agrin models shown in this study are available upon request.

Statistical Analysis

The data for all experiments were analyzed using ANOVA and Tukey's post-test (GraphPad Prism8, San Diego, CA), and *n* refers to the number of independent transfection or pulldown experiments. In all graphs, the bars represent the mean and error bars represent the SEM, and individual data points are superimposed to indicate the spread of data.

Supplementary Material

Supplementary Material is available at *HMG* online.

Acknowledgements

We thank Drs Steven Burden (NYU) and Joachim Herz (UT Southwestern) for their gifts of LRP4 expression constructs.

Conflict of Interest. None declared.

Funding

National Institutes of Health (R01NS049117 to R.M.).

References

1. Engel, A.G., Shen, X.M., Selcen, D. and Sine, S.M. (2015) Congenital myasthenic syndromes: pathogenesis, diagnosis, and treatment. *Lancet Neurol.*, **14**, 461.
2. Rodriguez Cruz, P.M., Palace, J. and Beeson, D. (2014) Inherited disorders of the neuromuscular junction: an update. *J. Neurol.*, **261**, 2234–2243.
3. Muller, J.S., Mihaylova, V., Abicht, A. and Lochmuller, H. (2007) Congenital myasthenic syndromes: spotlight on genetic defects of neuromuscular transmission. *Expert Rev. Mol. Med.*, **9**, 1–20.
4. Maselli, R.A., Arredondo, J., Ferns, M.J. and Wollmann, R.L. (2012) Synaptic basal lamina-associated congenital myasthenic syndromes. *Ann. N. Y. Acad. Sci.*, **1275**, 36–48.
5. Burden, S.J., Yumoto, N. and Zhang, W. (2013) The role of MuSK in synapse formation and neuromuscular disease. *Cold Spring Harb. Perspect. Biol.*, **5**, a009167.
6. Wu, H., Xiong, W.C. and Mei, L. (2010) To build a synapse: signaling pathways in neuromuscular junction assembly. *Development*, **137**, 1017–1033.
7. Burden, S.J., Huijbers, M.G. and Remedio, L. (2018) Fundamental molecules and mechanisms for forming and maintaining neuromuscular synapses. *Int. J. Mol. Sci.*, **19**, 490.
8. Gautam, M., Noakes, P.G., Moscoso, L., Rupp, F., Scheller, R.H., Merlie, J.P. and Sanes, J.R. (1996) Defective neuromuscular synaptogenesis in agrin-deficient mutant mice. *Cell*, **85**, 525–535.
9. DeChiara, T.M., Bowen, D.C., Valenzuela, D.M., Simmons, M.V., Poueymirou, W.T., Thomas, S., Kinetz, E., Compton, D.L., Rojas, E., Park, J.S. *et al.* (1996) The receptor tyrosine kinase MuSK is required for neuromuscular junction formation in vivo. *Cell*, **85**, 501–512.
10. Okada, K., Inoue, A., Okada, M., Murata, Y., Kakuta, S., Jigami, T., Kubo, S., Shiraishi, H., Eguchi, K., Motomura, M. *et al.* (2006) The muscle protein Dok-7 is essential for neuromuscular synaptogenesis. *Science*, **312**, 1802–1805.
11. Weatherbee, S.D., Anderson, K.V. and Niswander, L.A. (2006) LDL-receptor-related protein 4 is crucial for formation of the neuromuscular junction. *Development*, **133**, 4993–5000.
12. Hesser, B.A., Henschel, O. and Witzemann, V. (2006) Synapse disassembly and formation of new synapses in postnatal muscle upon conditional inactivation of MuSK. *Mol. Cell. Neurosci.*, **31**, 470–480.
13. Butikofer, L., Zurlinden, A., Bolliger, M.F., Kunz, B. and Sonderegger, P. (2011) Destabilization of the neuromuscular junction by proteolytic cleavage of agrin results in precocious sarcopenia. *FASEB J.*, **25**, 4378–4393.
14. Samuel, M.A., Valdez, G., Tapia, J.C., Lichtman, J.W. and Sanes, J.R. (2012) Agrin and synaptic laminin are required to maintain adult neuromuscular junctions. *PLoS One*, **7**, e46663.
15. Hopf, C. and Hoch, W. (1997) Heparin inhibits acetylcholine receptor aggregation at two distinct steps in the agrin-induced pathway. *Eur. J. Neurosci.*, **9**, 1170–1177.
16. Gesemann, M., Cavalli, V., Denzer, A.J., Brancaccio, A., Schumacher, B. and Ruegg, M.A. (1996) Alternative splicing of agrin alters its binding to heparin, dystroglycan, and the putative agrin receptor. *Neuron*, **16**, 755–767.
17. O'Toole, J.J., Deyst, K.A., Bowe, M.A., Nastuk, M.A., McKechnie, B.A. and Fallon, J.R. (1996) Alternative splicing of agrin regulates its binding to heparin alpha-dystroglycan, and the cell surface. *Proc. Natl. Acad. Sci. U. S. A.*, **93**, 7369–7374.
18. Zhang, B., Luo, S., Wang, Q., Suzuki, T., Xiong, W.C. and Mei, L. (2008) LRP4 serves as a coreceptor of agrin. *Neuron*, **60**, 285–297.
19. Kim, N., Stiegler, A.L., Cameron, T.O., Hallock, P.T., Gomez, A.M., Huang, J.H., Hubbard, S.R., Dustin, M.L. and Burden, S.J. (2008) Lrp4 is a receptor for agrin and forms a complex with MuSK. *Cell*, **135**, 334–342.
20. Burgess, R.W., Nguyen, Q.T., Son, Y.J., Lichtman, J.W. and Sanes, J.R. (1999) Alternatively spliced isoforms of nerve- and muscle-derived agrin: their roles at the neuromuscular junction. *Neuron*, **23**, 33–44.
21. Iozzo, R.V., Zoeller, J.J. and Nystrom, A. (2009) Basement membrane proteoglycans: modulators par excellence of cancer growth and angiogenesis. *Mol. Cells*, **27**, 503–513.
22. McCarthy, K.J. (2015) The basement membrane proteoglycans perlecan and agrin: something old, something new. *Curr. Top. Membr.*, **76**, 255–303.
23. Huze, C., Bauche, S., Richard, P., Chevessier, F., Goillot, E., Gaudon, K., Ben Ammar, A., Chaboud, A., Grosjean, I., Lecuyer, H.A. *et al.* (2009) Identification of an agrin mutation that causes congenital myasthenia and affects synapse function. *Am. J. Hum. Genet.*, **85**, 155–167.
24. Xi, J., Yan, C., Liu, W.W., Qiao, K., Lin, J., Tian, X., Wu, H., Lu, J., Wong, L.J., Beeson, D. *et al.* (2017) Novel SEA and LG2 Agrin mutations causing congenital myasthenic syndrome. *Orphanet J. Rare Dis.*, **12**, 182.
25. Zhang, Y., Dai, Y., Han, J.N., Chen, Z.H., Ling, L., Pu, C.Q., Cui, L.Y. and Huang, X.S. (2017) A novel AGRN mutation leads to congenital myasthenic syndrome only affecting limb-girdle muscle. *Chin Med J (Engl)*, **130**, 2279–2282.
26. Karakaya, M., Ceyhan-Birsoy, O., Beggs, A.H. and Topaloglu, H. (2017) A novel missense variant in the AGRN gene; congenital myasthenic syndrome presenting with head drop. *J. Clin. Neuromuscul. Dis.*, **18**, 147–151.
27. Nicole, S., Chaouch, A., Torbergsen, T., Bauche, S., de Bruyckere, E., Fontenille, M.J., Horn, M.A., van Ghelue, M., Loseth, S., Issop, Y. *et al.* (2014) Agrin mutations lead to a congenital myasthenic syndrome with distal muscle weakness and atrophy. *Brain*, **137**, 2429–2443.

28. Maselli, R.A., Fernandez, J.M., Arredondo, J., Navarro, C., Ngo, M., Beeson, D., Cagney, O., Williams, D.C., Wollmann, R.L., Yarov-Yarovoy, V. *et al.* (2012) LG2 agrin mutation causing severe congenital myasthenic syndrome mimics functional characteristics of non-neural (z-) agrin. *Hum. Genet.*, **131**, 1123–1135.
29. Lieth, E. and Fallon, J.R. (1993) Muscle agrin: neural regulation and localization at nerve-induced acetylcholine receptor clusters. *J. Neurosci.*, **13**, 2509–2514.
30. Ferns, M.J., Campanelli, J.T., Hoch, W., Scheller, R.H. and Hall, Z. (1993) The ability of agrin to cluster AChRs depends on alternative splicing and on cell surface proteoglycans. *Neuron*, **11**, 491–502.
31. Zong, Y. and Jin, R. (2013) Structural mechanisms of the agrin-LRP4-MuSK signaling pathway in neuromuscular junction differentiation. *Cell. Mol. Life Sci.*, **70**, 3077–3088.
32. Gesemann, M., Denzer, A.J. and Ruegg, M.A. (1995) Acetylcholine receptor aggregating activity of agrin isoforms and mapping of the active site. *J. Cell Biol.*, **128**, 625–636.
33. Jacobson, C., Montanaro, F., Lindenbaum, M., Carbonetto, S. and Ferns, M. (1998) alpha-Dystroglycan functions in acetylcholine receptor aggregation but is not a coreceptor for agrin–MuSK signaling. *J. Neurosci.*, **18**, 6340–6348.
34. Cornish, T., Chi, J., Johnson, S., Lu, Y. and Campanelli, J.T. (1999) Globular domains of agrin are functional units that collaborate to induce acetylcholine receptor clustering. *J. Cell Sci.*, **112**, 1213–1223.
35. Reissner, C., Runkel, F. and Missler, M. (2013) Neurexins. *Genome Biol.*, **14**, 213.
36. Hoch, W., Ferns, M., Campanelli, J.T., Hall, Z.W. and Scheller, R.H. (1993) Developmental regulation of highly active alternatively spliced forms of agrin. *Neuron*, **11**, 479–490.
37. Hoch, W., Campanelli, J.T., Harrison, S. and Scheller, R.H. (1994) Structural domains of agrin required for clustering of nicotinic acetylcholine receptors. *EMBO J.*, **13**, 2814–2821.
38. Anselmo, A., Lauranzano, E., Soldani, C., Ploia, C., Angioni, R., D'Amico, G., Sarukhan, A., Mazzon, C. and Viola, A. (2016) Identification of a novel agrin-dependent pathway in cell signaling and adhesion within the erythroid niche. *Cell Death Differ.*, **23**, 1322–1330.
39. Mazzon, C., Anselmo, A., Cibella, J., Soldani, C., Destro, A., Kim, N., Roncalli, M., Burden, S.J., Dustin, M.L., Sarukhan, A. *et al.* (2011) The critical role of agrin in the hematopoietic stem cell niche. *Blood*, **118**, 2733–2742.
40. Mazzon, C., Anselmo, A., Soldani, C., Cibella, J., Ploia, C., Moalli, F., Burden, S.J., Dustin, M.L., Sarukhan, A. and Viola, A. (2012) Agrin is required for survival and function of monocytic cells. *Blood*, **119**, 5502–5511.
41. Khan, A.A., Bose, C., Yam, L.S., Soloski, M.J. and Rupp, F. (2001) Physiological regulation of the immunological synapse by agrin. *Science*, **292**, 1681–1686.
42. Jury, E.C. and Kabouridis, P.S. (2010) New role for agrin in T cells and its potential importance in immune system regulation. *Arthritis Res. Ther.*, **12**, 205.
43. Eldridge, S., Nalesso, G., Ismail, H., Vicente-Greco, K., Kabouridis, P., Ramachandran, M., Niemeier, A., Herz, J., Pitzalis, C., Perretti, M. *et al.* (2016) Agrin mediates chondrocyte homeostasis and requires both LRP4 and alpha-dystroglycan to enhance cartilage formation *in vitro* and *in vivo*. *Ann. Rheum. Dis.*, **75**, 1228–1235.
44. Hausser, H.J., Ruegg, M.A., Brenner, R.E. and Ksiazek, I. (2007) Agrin is highly expressed by chondrocytes and is required for normal growth. *Histochem. Cell Biol.*, **127**, 363–374.
45. Steiner, E., Enzmann, G.U., Lyck, R., Lin, S., Ruegg, M.A., Kroger, S. and Engelhardt, B. (2014) The heparan sulfate proteoglycan agrin contributes to barrier properties of mouse brain endothelial cells by stabilizing adherens junctions. *Cell Tissue Res.*, **358**, 465–479.
46. Ksiazek, I., Burkhardt, C., Lin, S., Seddik, R., Maj, M., Bezakova, G., Jucker, M., Arber, S., Caroni, P., Sanes, J.R. *et al.* (2007) Synapse loss in cortex of agrin-deficient mice after genetic rescue of perinatal death. *J. Neurosci.*, **27**, 7183–7195.
47. Huang, M.L., Tota, E.M., Lucas, T.M. and Godula, K. (2018) Influencing early stages of neuromuscular junction formation through glycocalyx engineering. *ACS Chem. Neurosci.*, **19**, 3086–3093.
48. Hacker, U., Nybakken, K. and Perrimon, N. (2005) Heparan sulphate proteoglycans: the sweet side of development. *Nat. Rev. Mol. Cell Biol.*, **6**, 530–541.
49. Bernfield, M., Gotte, M., Park, P.W., Reizes, O., Fitzgerald, M.L., Lincecum, J. and Zako, M. (1999) Functions of cell surface heparan sulfate proteoglycans. *Annu. Rev. Biochem.*, **68**, 729–777.
50. Brandan, E. and Gutierrez, J. (2013) Role of skeletal muscle proteoglycans during myogenesis. *Matrix Biol.*, **32**, 289–297.
51. Zhang, W., Coldefy, A.S., Hubbard, S.R. and Burden, S.J. (2011) Agrin binds to the N-terminal region of Lrp4 protein and stimulates association between Lrp4 and the first immunoglobulin-like domain in muscle-specific kinase (MuSK). *J. Biol. Chem.*, **286**, 40624–40630.
52. Chen, F., Venugopal, V., Murray, B. and Rudenko, G. (2011) The structure of neurexin 1alpha reveals features promoting a role as synaptic organizer. *Structure*, **19**, 779–789.
53. Gubbiotti, M.A., Neill, T. and Iozzo, R.V. (2017) A current view of perlecan in physiology and pathology: a mosaic of functions. *Matrix Biol.*, 57, 285–58, 298.
54. Bender, B.J., Cisneros, A. 3rd, Duran, A.M., Finn, J.A., Fu, D., Lokits, A.D., Mueller, B.K., Sangha, A.K., Sauer, M.F., Sevy, A.M. *et al.* (2016) Protocols for molecular modeling with Rosetta3 and RosettaScripts. *Biochemistry*, **55**, 4748–4763.
55. Alford, R.F., Leaver-Fay, A., Jeliazkov, J.R., O'Meara, M.J., DiMaio, F.P., Park, H., Shapovalov, M.V., Renfrew, P.D., Mulligan, V.K., Kappel, K. *et al.* (2017) The Rosetta all-atom energy function for macromolecular modeling and design. *J. Chem. Theory Comput.*, **13**, 3031–3048.
56. Rohl, C.A., Strauss, C.E., Misura, K.M. and Baker, D. (2004) Protein structure prediction using Rosetta. *Methods Enzymol.*, **383**, 66–93.
57. Wang, C., Bradley, P. and Baker, D. (2007) Protein-protein docking with backbone flexibility. *J. Mol. Biol.*, **373**, 503–519.
58. Bonneau, R., Strauss, C.E., Rohl, C.A., Chivian, D., Bradley, P., Malmstrom, L., Robertson, T. and Baker, D. (2002) De novo prediction of three-dimensional structures for major protein families. *J. Mol. Biol.*, **322**, 65–78.
59. Nivon, L.G., Moretti, R. and Baker, D. (2013) A Pareto-optimal refinement method for protein design scaffolds. *PLoS One*, **8**, e59004.
60. Conway, P., Tyka, M.D., Dimaio, F., Konerding, D.E. and Baker, D. (2014) Relaxation of backbone bond geometry improves protein energy landscape modeling. *Protein Sci.*, **23**, 47–55.
61. Tyka, M.D., Keedy, D.A., Andre, I., Dimaio, F., Song, Y., Richardson, D.C., Richardson, J.S. and Baker, D. (2011) Alternate states of proteins revealed by detailed energy landscape mapping. *J. Mol. Biol.*, **405**, 607–618.

62. Khatib, F., Cooper, S., Tyka, M.D., Xu, K., Makedon, I., Popovic, Z., Baker, D. and Players, F. (2011) Algorithm discovery by protein folding game players. *Proc. Natl. Acad. Sci. USA*, **108**, 18949–18953.

63. Pettersen, E.F., Goddard, T.D., Huang, C.C., Couch, G.S., Greenblatt, D.M., Meng, E.C. and Ferrin, T.E. (2004) UCSF Chimera—a visualization system for exploratory research and analysis. *J. Comput. Chem.*, **25**, 1605–1612.